Proceedings of the Canadian Society for Mechanical Engineering International Congress
32nd Annual Conference of the Computational Fluid Dynamics Society of Canada
Canadian Society of Rheology Symposium
CSME-CFDSC-CSR 2025
May 25–28, 2025, Montréal, Québec, Canada

CORROSION PERFORMANCE OF BORONIZED MARTENSITIC STAINLESS STEELS

Nirupama Mohan[1, 2*], Gajanana P Chaudhari[1],
[1]Metallurgical and material engineering department, IIT- Roorkee, Roorkee, India 1
[2]Department of Mechanical Engineering, BMS College of Engineering, Bengaluru, India 2
*nirupamamohan.mech@bmsce.ac.in

Abstract—13Cr-4Ni and 16Cr-5Ni martensite stainless steels were pack boronized at 950 and 1000 ℃. These samples were further tempered at 600 ℃ for 2 h. Pack boronizing lead to the development of boride layer on the MSS Substrate. Immersion tests were conducted in 0.1 M H_2SO_4 and 0.06 M HCl media. SEM micrographs reveal the surface morphology of all the samples post immersion tests. Potentiodynamic polarization tests were also conducted in 0.6 M NaCl solution. Boronized samples show a reduction in weight loss as compared to their bare counterparts in the given immersion media. However, the polarization curves demonstrate inferior corrosion performance of the boronized samples.

Keywords-boronizing; martensite stainless steel; corrosion

I. INTRODUCTION

Martensite stainless-steel grades (MSS) such as 13Cr-4Ni and 16Cr-5Ni are used in the fabrication of hydro-turbine components such as blades and engine components [1]. MSS grades are preferred owing to their high strength, low temperature ductility, toughness and corrosion resistance properties [2][3]. The metastable phase of martensite is achieved by quenching from the austenite phase which imparts high hardness to these grades of steels. Martensitic stainless steel (MSS) is prone to pitting corrosion in environments containing aggressive anions like chloride ions (Cl-). These ions can penetrate the passive protective film on the material's surface, leading to localized dissolution [2]. In hydro turbine blades, this issue is further exacerbated by the continuous impact of silt particles in freshwater, which repeatedly disrupts the passive film [3]. Although chromium in MSS promotes passivation, the silt-induced damage impairs the material's ability to repassivate effectively. Additionally, microstructural defects and pores further accelerate material degradation, increasing the risk of component failure. While many studies focus on enhancing surface hardness to mitigate erosion and cavitation, it is crucial to also investigate the electrochemical interactions, as the corrosive environment can significantly intensify material deterioration, both independently and in combination with cavitation-erosion phenomena [4][5]. Studies have shown that surface treatments can enhance both hardness and corrosion resistance [6-9]. Carburizing, nitriding and boronizing are some of the common techniques employed [10-12]. Among these techniques, boronizing is the simplest and cost-effective method which increases the hardness as well as the corrosion resistance of the substrate material [13]. Boronizing is a diffusion coating method where the B atoms occupy the interstitial spaces and form borides with the substrate alloy. Generally, boronizing steel yields a layer comprising of iron borides (FeB, Fe_2B) and in some high alloy content steels additional borides are also reported [14]. Pack boronizing method is most often used for the boronizing of stainless steels. For boronizing steels, the process parameters of; boronizing temperature and duration are usually selected in the range of 850-1050 ℃ and duration of 4 - 8 h respectively. Process optimization specific to the substrate alloy is crucial in obtaining the requisite layer thickness and composition [15]. Several studies have shown the effect of boronizing on the corrosion resistance of various steel grades. Kayali et al boronized AISI 316L stainless steel for 2 and 6 h at 800 and 900 ℃ respectively and reported that boronizing enhances the corrosion resistance in HCl acidic medium [1]. Yusuf et al boronized AISI 316L stainless steel 2 and 6 h at 800 and 900 ℃ respectively and reported that boronizing caused a decline in the corrosion current density values in simulated body fluid medium [2]. Cetin et al boronized AISI 904L at 900, 1000 and 1100 °C for 2, 4, and 6 h and reported that boronizing did not effectively enhance corrosion resistance in NaCl medium but the values of corrosion parameters obtained were comparable with AISI 316 stainless steel [3]. Naemchanthara et al boronized AISI 304 stainless steel 800 °C, 850 °C, and 900 °C for 2 hours under an argon atmosphere and reported an enhancement in the corrosion behavior of the boronized SS in NaCl medium [4]. From the available literature it can deduced that most studies focus on boronizing of austenite grades of stainless steels and the corrosion performance is influenced by various parameters. Also, limited studies are available about the corrosion performance of boronized MSS. Therefore, the present work focuses on assessing the corrosion behavior of 13Cr-4Ni and 16Cr-5Ni MSS for the processing parameters chosen in both acidic and chloride medium. The SEM and XRD analysis will help in comprehending the degradation behavior and surface chemistry of the corroded samples.

II. MATERIALS AND METHODS

A. Material processing

As cast 13Cr-4Ni and 16Cr-5Ni MSS were procured from BHEL, Haridwar, India. Their composition was assessed using wavelength dispersive X-ray fluorescence spectroscopy and is given in Table 1. Powder pack boronizing (pack composition: Silicon carbide 90 wt%, Potassium tetra fluoroborate 5 wt% and Boron carbide 5 wt%) technique was used to boronize the samples at 950 and 1000 ºC for 6 h followed by tempering at 600 C for 2 h. Figure 1. shows the cross-section of the boronized sample. The important features that can be noted are i. cross-section can be clearly separated into three zones: the boronized layer, intermediary diffusion zone and substrate, ii. thickness of the boronized layer is non-uniform and ranges between 40-90 µm, iii. FeB is seen in the exterior and Fe_2B is seen toward the interior on the boronized layer and iv. Pores are seen but micro-cracks are not seen in the boronized layer. The process parameters (boronizing temperature and duration) were chosen to achieve optimum combination of layer thickness, morphology and mechanical properties of the boronized layer which was reported in a previous study [16]. The details of layer thickness and composition are tabulated in table 2 [16].

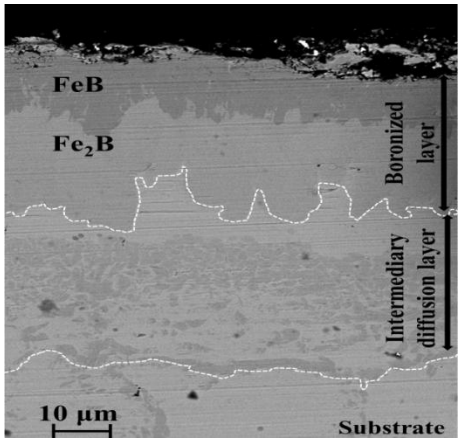

Figure 1. SEM micrograph of 13Cr-4Ni MSS boronized at 950 ℃

B. Electrochemical behviour

Potentiodynamic polarization was performed using Gamry 1000® potentiostat at ambient temperature in 0.6 M NaCl solution. An initial delay of 1800 s was provided to achieve stabilization before the polarization tests. Saturated Calomel Electrode was used as reference electrode; a platinum mesh counter electrode was employed and the boronized sample with an exposed area of 0.785 cm^2 was the working electrode. Standard scan rate of 0.167 mVs-1 (both forward and backward scan) and a peak current density of 10 mA/cm^2 were used for polarization tests. Immersion tests were performed in two acidic media: 0.06 M HCl (non-oxidizing acid) and 0.1M H_2SO_4 (oxidizing acid) at room temperature for a duration of 72 h as per ASTM G31 standard and the weight loss was measured at a regular interval of 6 h. Samples were immersed in 100 ml of 5 vol% of 0.06 M HCl and 0.1 M H_2SO_4 solution separately. After every 6 h interval the sample was scrubbed gently using soft wire brush, washed with soap water and rinsed in distilled water before measuring weight loss. For immersion tests, samples of 10 X 10 X 2 mm were cut from the billets and for the electro-chemical tests circular sample of 30 X 5 mm were used. The samples were polished using various grit sizes of silicon carbide abrasive papers and boronized before subjecting to electro-chemical tests. The corrosion rate of the samples subjected to immersion test was evaluated using the equation:

$$C.R = 87.6 \times (W/DAT). \quad (1)$$

where W, D, A and T are weight loss (mg), density (g/cm^{-3}), area of the sample (cm^2) and time of exposure (h) respectively.

TABLE I. CHEMICAL COMPOSITION (IN WT%)

Material	Elements					
	C	***Si***	***Cr***	***Ni***	***Mo***	***Fe***
13Cr-4Ni MSS	0.020	0.84	13.2	3.5	0.55	Balance
16Cr-5Ni MSS	0.021	1.43	15.9	4.9	0.99	Balance

TABLE II. LAYER THICKNESS AND COMPOSITION OF BORONIZED LAYER [16]

Parameters	Material Processing			
	13Cr-4Ni 950 ℃	***16Cr-5Ni 950 ℃***	***13Cr-4Ni 1000 ℃***	***16Cr-5Ni 1000 ℃***
Layer thickness (µm)	40-55	75-90	35-50	55-70
Composition	FeB, Fe_2B	FeB, Fe2B, Cr_2B, Ni_2B	FeB, Fe2B, Ni_2B	FeB, Fe2B, CrB, Cr_2B, NiB, Ni_2B

C. Microstructural characterization

The imaging of the samples (both bare and boronized) subject to immersion tests was accomplished using FEI Quanta 200F scanning electron microscope (SEM) equipped with energy dispersive spectroscopy (EDS). A Rigaku SmartLab® X-ray diffractometer was used to identify the phases present on the immersion tested samples (both bare and boronized).

III. RESULTS AND DISCUSSIONS

A. Immersion test

Immersion tests were conducted on the bare and boronized 13Cr-4Ni and 16Cr-5Ni MSS samples to measure the weight loss occurring in two acidic media; 0.06 M HCl and 0.1 M H_2SO_4 and are shown in Figs. 2 and 3 (a-b). The weight loss of the samples varied from 1.1118 to 0.9854 mg/cm^2 and 0.735 to 0.065 mg/cm^2 in 0.1 M H_2SO_4 while 0.6354 to 0.565 mg/cm^2 and 0.0135 to 0.0095 mg/cm^2 in 0.06 M HCl for bare and boronized samples, respectively. Maximum weight loss was observed for bare samples in comparison with boronized samples in both acidic media. Also, the weight loss increased in 0.1 M H_2SO_4 as compared to 0.06 M HCl for all the samples. The trend of the weight loss curves is almost linear (weight loss increases over time). The important observations that can be made from the weight loss curves are that for both grades of

MSS, boronized samples show significant reduction in weight loss over bare samples, in comparison with boronized 13Cr-4Ni MSS, 16Cr-5Ni MSS shows lesser weight loss and among the boronizing temperature of 950 and 1000 °C, both grades of MSS boronized at 1000 °C show lesser weight loss. The corrosion rates measured from the weight loss values for boronized 13Cr-4Ni and 16Cr-5Ni MSS at 950 and 1000 °C are tabulated as shown in table 5. The calculated values are consistent with the observations made from Figs. 2 and 3 (a-b). Bare samples have higher corrosion rates, boronized 16Cr-5Ni MSS shows reduction in corrosion rates in comparison with13Cr-4Ni MSS and 16Cr-5Ni MSS boronized at 1000 °C shows the least corrosion rate in both acidic media.

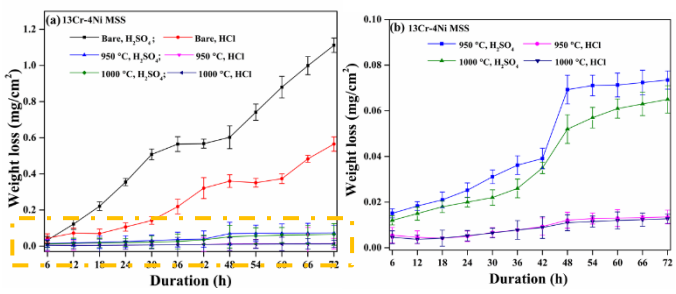

Figure 2. Weight loss in acidic (0.06M HCl, 0.1M H_2SO_4) media of (a) all samples and (b) enlarged portion of Fig (a) consisting of only boronized specimens of 13Cr-4Ni MSS

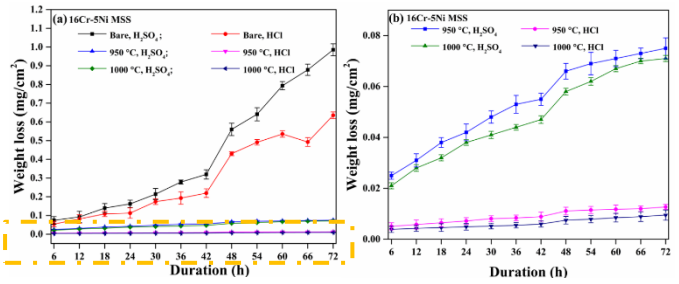

Figure 3. Weight loss in acidic (0.06M HCl, 0.1M H_2SO_4) media of (a) all samples and (b) enlarged portion of Fig (a) consisting of only boronized specimens of 16Cr-5Ni MSS

TABLE III. CORROSION RATE

Test condition		Corrosion rate (mm/yr)		
		Bare	***950 °C***	***1000 °C***
H_2SO_4	13Cr-4 Ni MSS	0.1713	0.0116	0.0112
	16Cr-5Ni MSS	0.1522	0.0114	0.0101
HCl	13Cr-4 Ni MSS	0.0983	0.0021	0.0019
	16Cr-5Ni MSS	0.0872	0.0019	0.0014

SEM micrographs (Figs. 4 and 5 (a-f)) reveal that for the bare samples presence of large pits and corrosion scales are observed. However, for the boronized MSS grades micro-cracks and cracks are observed. The cracks are more pronounced when the samples are immersed in H_2SO_4 than in HCl, the effect of boronizing temperature has no effect on the corrosion mechanism irrespective of the acidic medium and similar features can be seen on both grades of boronized MSS and the attack of the 0.1 M H_2SO_4 on MSS grades boronized at 950 °C is severe in comparison with samples boronized at 1000 °C while the attack of 0.06 M HCl on the MSS grades at 950 and 1000 °C are similar. Further, the integrity of the boronized layer and the surface chemistry of the samples subject to immersion test was analyzed using XRD. For the boronized samples immersed in 0.1 M H_2SO_4, the spectra (Fig. 6(a)) reveal the prominent phases of Fe_2B, FeB, Fe_3O_4, Fe_2O_3 and CrO_3 and when immersed in 0.06 M HCl (Fig. 6(b)), Fe_2B, FeB, $FeCl_2$, Fe_2O_3, Fe_3O_4, CrO_3 and B_6O were observed. The presence of Fe_2B and FeB in all cases shows that irrespective of the acidic media the boronized layer is not compromised. Also, the careful comparison of the XRD results between i. boronized 13Cr-4Ni and 16Cr-5Ni MSS show several similarities, yet the oxide peaks are more prominent in the latter and ii. at boronizing temperature of 950 ºC minimal presence of Fe_2O_3 and Fe_3O_4 is seen as compared to 1000 ºC for both 13Cr-4Ni and 16Cr-5Ni MSS. These results are consistent with the weight loss seen in Figs. 2 and 3 (a-b). Kartal et al studied. effect of immersing borided DIN EN10130-99 and DC04 low carbon steel steel in various oxidizing and non-oxidizing acidic media and reported higher weight loss in H_2SO_4 due to severe pitting as compared to HCl media [5]. G. K. Kariofillis et al also studied the effect of specific acids (H_2SO4, HCl and HPO_3) on borided AISI H13 Steel and reported pitting to be the main degradation mechanism for samples immersed in H_2SO_4 [6].

In the present study, similar effects of acidic media on weight loss are observed but the corrosion mechanism of boronized samples is different. This is because the grades of steel used in afore mentioned studies contain a lower percentage of alloying elements, especially Cr and Ni which are pivotal in affecting the chemical interaction between the boronized layer and acidic media. The presence of chromium borides (Cr_2B, CrB) on the layer due to the precipitation of Cr from the solid solution causes intergranular attack which manifests as cracks on the surface. As the attack of acidic media continues these cracks become more pronounced and lead to degradation of the material. The corrosion mechanism of boronized MSS grades observed in both media (Figs. 4 and 5) shows no signs of pitting. However, increased corrosion resistance of the boronized MSS grades during immersion may be due to uniform kinetics of reaction. Also, NaCl salt solution, used as the electrolyte in cyclic polarization, increases the ionic conductivity; due to the presence of Cl- ions, attacks more aggressively and can penetrate protective passive films while acidic media (H_2SO_4 and HCl) aids passivation due to the presence of H^+ ions.

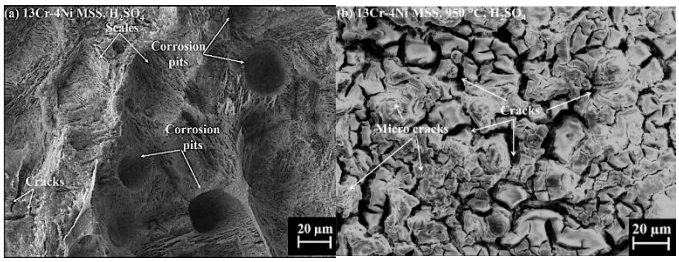

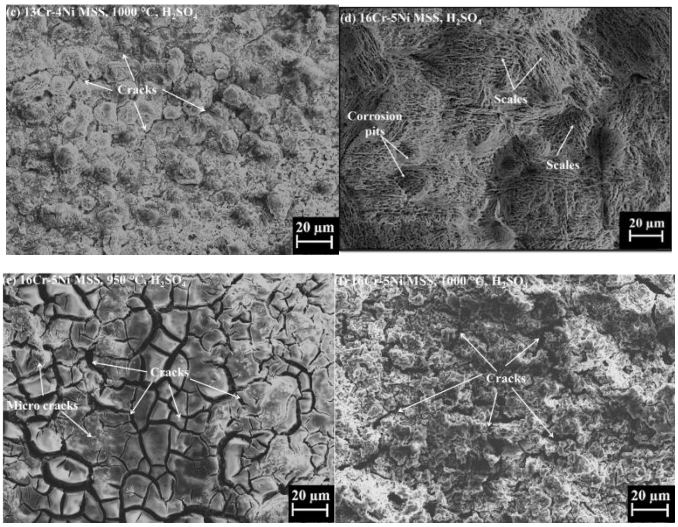

Figure 4. SEM images of surface of bare and boronized (a-c) 13Cr-4Ni and (d-f) 16Cr-5Ni MSS after immersion in 0.1 M H_2SO_4 solution for 6 h

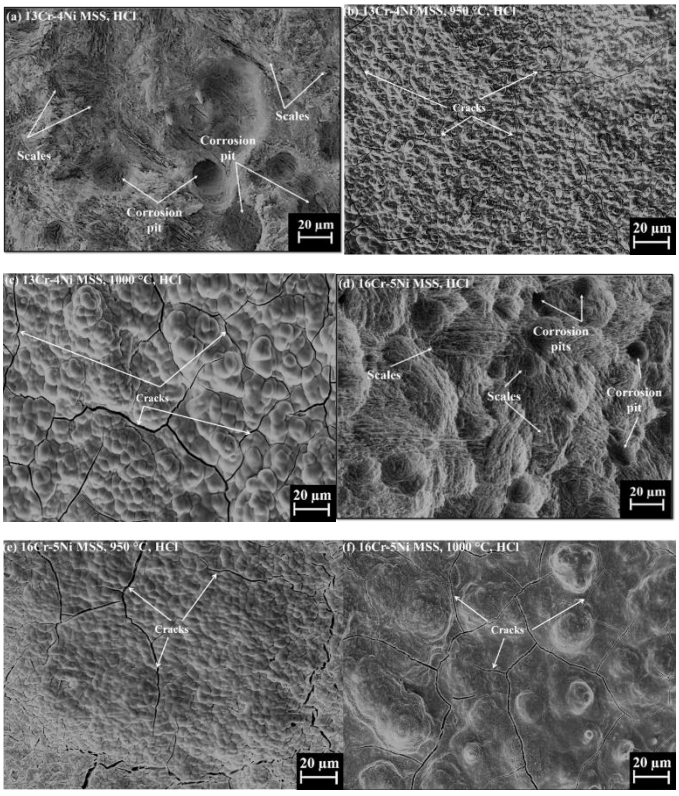

Figure 5. SEM images of surface of bare and boronized (a-c) 13Cr-4Ni and (d-f) 16Cr-5Ni MSS after immersion in 0.6 M HCl solution for 6 h

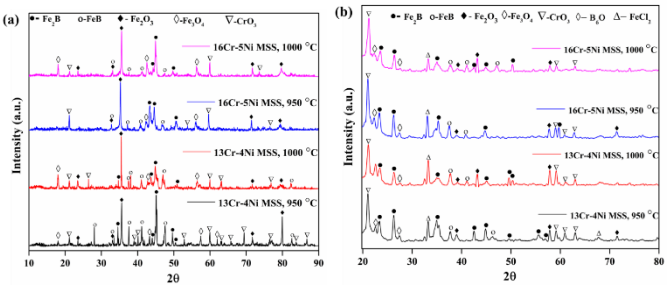

Figure 6. XRD analysis of boronized 13Cr-4Ni and 16Cr-5Ni MSS subject to immersion in **(a)** 0.1 M H_2SO_4 and **(b)** 0.06 M HCl

B. Potentiodynamic polarization test

The potentiodynamic polarization curves of the bare and boronized samples are as shown in Fig. 7. The corrosion potential (E_{corr}) and corrosion current density (I_{corr}) are also calculated from these curves. The E_{corr} values of boronized MSS is more active by atleast 200 mV and as high as 310 mV in comparison with their bare counterparts. The corrosion current density is also slightly higher for the boronized samples. The bare samples exhibit passivation tendencies while constant corrosion is observed in the case of boronized samples. For boronized samples, some electrochemical noise is observed in both the anodic and cathodic regions which is due to the constant repassivation of the metastable pits. Specifically, more electrochemical noise is observed in the case of 16Cr-5Ni MSS boronized at 950 ℃. In the cathode region, all samples show a diffusion-controlled regime which indicates that in the aerated NaCl solution, the I_{corr} values are determined by the oxygen reduction kinetics which serve as the rate limiting factor. In the anode region, the bare and boronized samples show varied behavior. In the anode region, the polarization curves of the bare samples initially demonstrate passivation tendencies with the E_{corr} values shifting towards nobler potentials up to 1µA/cm^2 beyond which the passive film ruptures and the corrosion current density constantly increases. However, boronized MSS does not show any passivation tendencies, and material corrodes constantly. The surface inhomogeneities in the boronized layer allows for electrochemical activity as the corrosion medium can penetrate beneath the boronized layer. Also, the possibility of partial sensitization during boronizing, and Cr tendency to form CrB and Cr_2B both of which leads to Cr depletion from the solid solution thereby limiting the passivation tendencies of boronized MSS and causes intergranular corrosion [22] .

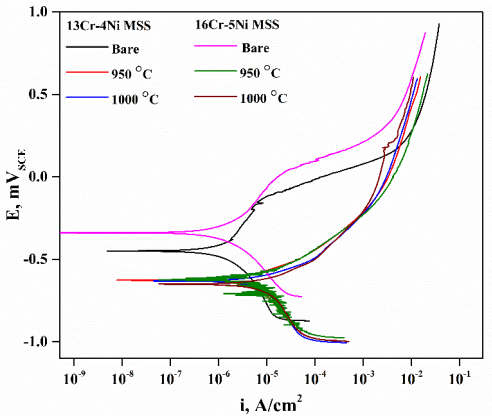

Figure 7. Potentiodynamic polarization curves of bare and boronized samples

TABLE IV. CORROSION PARAMETERS

Material		E_{corr}, mV_{SCE}	i_{corr}, $\mu A/cm^2$
13Cr-4Ni MSS	***Bare***	456 ± 22	0.6 ± 0.4
	Boronized at 950 °C	659 ± 12	6.7 ± 0.7
	Boronized at 1000 °C	664 ± 18	8.1 ± 0.3
16Cr-5Ni MSS	***Bare***	348 ± 24	0.9 ± 0.3
	Boronized at 950 °C	646 ± 15	4.3 ± 0.5
	Boronized at 1000 °C	658 ± 19	7.8 ± 0.2

IV. CONCLUSIONS

The corrosion resistance of boronized MSS grades was evaluated, and the important findings can be summarized as follows.

1. The electrochemical potential of the boronized MSS grades are lower than that of their bare counterparts due to their inability to passivate.
2. The immersion tests show lesser weight loss of boronized samples in both acidic media which could be attributed to uniform kinetics and passivation supported by the H^+ ions and corrosion products.
3. The values of I_{corr} are much higher for the boronized samples due to uniform corrosion of the boronized samples.

ACKNOWLEDGMENT

The authors would like to thank BMS College of Engineering, Bengaluru, India for the opportunity. The authors are also thankful to QIP, IIT- Roorkee for administrative facilitation in carrying out the present work.

REFERENCES

[1] B. Kishor, G.P. Chaudhari, S.K. Nath, Slurry erosion behaviour of thermomechanically treated 16Cr5Ni stainless steel, Tribology International 119 (2018) 411–418. https://doi.org/10.1016/j.triboint.2017.11.025.

[2] F. Yuan, G. Wei, S. Gao, S. Lu, H. Liu, S. Li, X. Fang, Y. Chen, Tuning the pitting performance of a Cr-13 type martensitic stainless steel by tempering time, Corrosion Science 203 (2022) 110346. https://doi.org/10.1016/j.corsci.2022.110346.

[3] R.K. Mohanta, T.R. Chelliah, S. Allamsetty, A. Akula, R. Ghosh, Sources of vibration and their treatment in hydro power stations-A review, Engineering Science and Technology, an International Journal 20 (2017) 637–648. https://doi.org/10.1016/j.jestch.2016.11.004.

[4] E. Quaranta, P. Davies, Emerging and Innovative Materials for Hydropower Engineering Applications: Turbines, Bearings, Sealing, Dams and Waterways, and Ocean Power, Engineering 8 (2022) 148–158. https://doi.org/10.1016/j.eng.2021.06.025.

[5] Md.A. Islam, J. (Jimmy) Jiang, Y. Xie, Optimizing material selection: A study of erosion-corrosion performance in homogeneous and carbide-containing materials, Wear 536–537 (2024) 205181. https://doi.org/10.1016/j.wear.2023.205181.

[6] Z. Xing, Z. Feng, Y. Wu, Y. Lu, Y. Duan, S. Zheng, M. Peng, M. Li, Y. Wu, Growth kinetics and corrosion properties of pack-borided Ti-5Al-2.5Sn alloy, Surface and Coatings Technology 473 (2023) 130003. https://doi.org/10.1016/j.surfcoat.2023.130003.

[7] S. Siddique, A.A. Bernussi, S.W. Husain, M. Yasir, Enhancing structural integrity, corrosion resistance and wear properties of Mg alloy by heat treated cold sprayed Al coating, Surface and Coatings Technology 394 (2020) 125882. https://doi.org/10.1016/j.surfcoat.2020.125882.

[8] S. Alkan, A. Günen, M. Gülen, M.S. Gök, Effect of boriding on tribocorrosion behaviour of HSLA offshore mooring chain steel, Surface and Coatings Technology 476 (2024) 130276. https://doi.org/10.1016/j.surfcoat.2023.130276.

[9] U. Gürol, Y. Altınay, A. Günen, Ö.S. Bölükbaşı, M. Koçak, G. Çam, Effect of powder-pack aluminizing on microstructure and oxidation resistance of wire arc additively manufactured stainless steels, Surface and Coatings Technology 468 (2023) 129742. https://doi.org/10.1016/j.surfcoat.2023.129742.

[10] P.M. Reinders, G. Bräuer, A model to predict the s-phase thickness and the change in corrosion behavior toward H2SO4 of 316L austenitic stainless steel after plasma nitriding, Surface and Coatings Technology 475 (2023) 130135. https://doi.org/10.1016/j.surfcoat.2023.130135.

[11] M. Yazıcı, O. Çomaklı, T. Yetim, A.F. Yetim, A. Çelik, Investigation of mechanical, tribological and magnetic properties after plasma nitriding of AISI 316L stainless steel produced with different orientations angles by selective laser melting, Surface and Coatings Technology 467 (2023) 129676. https://doi.org/10.1016/j.surfcoat.2023.129676.

[12] I. Campos-Silva, E.J. Hernández-Ramirez, A. Contreras-Hernández, J.L. Rosales-Lopez, E. Valdez-Zayas, I. Mejía-Caballero, J. Martínez-Trinidad, Pulsed-DC powder-pack boriding: Growth kinetics of boride layers on an AISI 316 L stainless steel and Inconel 718 superalloy, Surface and Coatings Technology 421 (2021) 127404. https://doi.org/10.1016/j.surfcoat.2021.127404.

[13] A. Günen, U. Gürol, M. Koçak, G. Çam, A new approach to improve some properties of wire arc additively manufactured stainless steel components: Simultaneous homogenization and boriding, Surface and Coatings Technology 460 (2023) 129395. https://doi.org/10.1016/j.surfcoat.2023.129395.

[14] R.A. García-León, J. Martínez-Trinidad, I. Campos-Silva, U. Figueroa-López, A. Guevara-Morales, Development of tribological maps on borided AISI 316L stainless steel under ball-on-flat wet sliding conditions, Tribology International 163 (2021) 107161. https://doi.org/10.1016/j.triboint.2021.107161.

[15] N. Mohan, G. Chaudhari, Microstructural evolution and mechanical behaviour of boronized martensitic stainless steels, Surface Engineering 38 (2022) 552–561. https://doi.org/10.1080/02670844.2022.2113612.

[16] Y. Kayali, A. Büyüksağiş, I. Güneş, and Y. Yalçin, "Investigation of corrosion behaviors at different solutions of boronized AISI 316L stainless steel," *Protection of Metals and Physical Chemistry of Surfaces*, vol. 49, no. 3, pp. 348–358, May 2013, doi: 10.1134/S2070205113030192.

[17] Y. Kayali, A. Büyüksaçiş, and Y. Yalçin, "Corrosion and wear behaviors of boronized AISI 316L stainless steel," *Metals and Materials International*, vol. 19, no. 5, pp. 1053–1061, 2013, doi: 10.1007/s12540-013-5019-x.

[18] M. Çetin, A. Günen, M. Kalkandelen, and M. S. Karakaş, "Microstructural, wear and corrosion characteristics of boronized AISI 904L superaustenitic stainless steel," *Vacuum*, vol. 187, p. 110145, May 2021, doi: 10.1016/j.vacuum.2021.110145.

[19] P. Naemchanthara and P. Juijerm, "Effects of Heat Treatment on Phase Transformation and Corrosion Resistance of Boride Layer on Austenitic Stainless Steel AISI 304," *Metallurgical and Materials Transactions B*, vol. 49, no. 5, pp. 2875–2880, Oct. 2018, doi: 10.1007/s11663-018-1337-1.

[20] G. Kartal, O. Kahvecioglu, and S. Timur, "Investigating the morphology and corrosion behavior of electrochemically borided steel," *Surf Coat Technol*, vol. 200, no. 11, pp. 3590–3593, Mar. 2006, doi: 10.1016/j.surfcoat.2005.02.210.

[21] G. K. Kariofillis, G. E. Kiourtsidis, and D. N. Tsipas, "Corrosion behavior of borided AISI H13 hot work steel," *Surf Coat Technol*, vol. 201, no. 1–2, pp. 19–24, 2006, doi: 10.1016/j.surfcoat.2005.10.025.

[22] N. Mohan, A. Kumar, and G. P. Chaudhari, "Effect of Boronizing on the Corrosion Resistance of Martensitic Stainless Steels," *J Mater Eng Perform*, 2024, doi: 10.1007/s11665-024-10188-0.